Physics Letters B 759 (2016) 342–348

Contents lists available at ScienceDirect

Physics Letters B

www.elsevier.com/locate/physletb

Kaluza–Klein gluon + jets associated production at the Large Hadron Collider

A.M. Iyer [a], F. Mahmoudi [b,c,*,1], N. Manglani [d,e], K. Sridhar [a]

[a] Department of Theoretical Physics, Tata Institute of Fundamental Research, Homi Bhabha Road, Colaba, Mumbai 400 005, India
[b] Univ Lyon, Univ Lyon 1, ENS de Lyon, CNRS, Centre de Recherche Astrophysique de Lyon UMR5574, F-69230 Saint-Genis-Laval, France
[c] Theoretical Physics Department, CERN, CH-1211 Geneva 23, Switzerland
[d] Department of Physics, University of Mumbai, Kalina, Mumbai 400098, India
[e] Shah and Anchor Kutchhi Engineering College, Mumbai 400088, India

ARTICLE INFO

Article history:
Received 25 February 2016
Received in revised form 18 April 2016
Accepted 30 May 2016
Available online 2 June 2016
Editor: G.F. Giudice

ABSTRACT

The Kaluza–Klein excitations of gluons offer the exciting possibility of probing bulk Randall–Sundrum (RS) models. In these bulk models either a custodial symmetry or a deformation of the metric away from AdS is invoked in order to deal with electroweak precision tests. Addressing both these models, we suggest a new channel in which to study the production of KK-gluons (g_{KK}): one where it is produced in association with one or more hard jets. The cross-section for the g_{KK} + jets channel is significant because of several contributing sub-processes. In particular, the 1-jet and the 2-jet associated processes are important because at these orders in QCD the qg and the gg initial states respectively come into play. We have performed a hadron-level simulation of the signal and present strategies to effectively extract the signal from what could potentially be a huge background. We present results for the kinematic reach of the LHC Run-II for different g_{KK} masses in bulk-RS models.

1. The bulk Randall–Sundrum model

The Randall–Sundrum model (RS model) [1] is a five-dimensional model with a warped metric and was proposed as a solution to the gauge-hierarchy problem. In this five-dimensional model, the fifth dimension y is compactified on an S^1/Z^2 orbifold of radius, R. At the fixed points of the orbifold, $y = 0$ and $y = \pi R \equiv L$, two branes – the UV and the IR brane respectively – are located.

One starts with a warped metric given as:

$$ds^2 = e^{-2A(y)}\eta_{\mu\nu}dx^\mu dx^\nu - dy^2 \tag{1}$$

and using a five-dimensional gravity action with a bulk cosmological constant Λ one can show that the solutions to the Einstein equation imply

$$A(y) = \pm k|y| \tag{2}$$

where $k^2 \equiv -\Lambda/12M^3$ with M being the Planck scale.

The Standard Model (SM) fields are all IR-localised and only the graviton fields access the bulk. The factor of $v/M \sim 10^{-16}$ (where v is the vacuum expectation value of the SM Higgs field) is generated by choosing a value of $kL \sim 30$ thereby stabilising the gauge hierarchy.

The problem, however, is that the suppression that one obtains for the Higgs vev materialises for all fields localised on the IR brane. Thus, mass scales which suppress dangerous higher-dimensional operators responsible for proton decay or neutrino masses also become small which spells a disaster for the RS model. One way out of this is to realise that to solve the gauge-hierarchy problem one needs to only localise the Higgs on the IR brane but all the other SM fields could be in the bulk [2–5]. In fact, even the Higgs need not be sharply localised on the IR brane but only somewhere close to it. In this way, it is possible to make viable variations of the RS model, now collectively known as Bulk RS models. These models yield a bonus: localising fermions at different positions in the bulk gives different overlaps of their profiles with the Higgs field, which is localised on or close to the IR brane. This gives rise in a natural way to the Yukawa-coupling hierarchy [4].

The AdS/CFT correspondence when worked out for a slice of AdS spacetime also provides both a motivation for and an understanding of bulk models. (For a review, see Ref. [6].) In fact,

* Corresponding author.
E-mail addresses: abhishek@theory.tifr.res.in (A.M. Iyer), nazila@cern.ch (F. Mahmoudi), namratam@physics.mu.ac.in (N. Manglani), sridhar@theory.tifr.res.in (K. Sridhar).

[1] Also at Institut Universitaire de France, 103 boulevard Saint-Michel, 75005 Paris, France.

http://dx.doi.org/10.1016/j.physletb.2016.05.090

this correspondence shows that the dual of the RS model with all the SM fields on the IR brane is a fully composite SM in four dimensions – a theory which we know does not survive in the face of extant experimental constraints. But when the SM fields are localised at different positions in the bulk, one ends up with a partially composite SM where the compositeness is primarily in the Higgs, the top and in the KK sector. Such a model is, in fact, a viable model as we will discuss in the following.

It is possible to construct a bulk-extension of the SM by having the gauge and fermion fields in the bulk, the Higgs localised on or near the IR brane and with a suitable mechanism to make the model successfully confront constraints from electroweak precision measurements [6]. Such a model has interesting features. Other than providing a framework for addressing the question of fermion mass hierarchy, it also naturally results in small mixing angles in the Cabibbo–Kobayashi–Maskawa (CKM) matrix, gauge-coupling universality and suppression of flavour-changing neutral currents to experimentally acceptable values [7–11].

Electroweak precision tests provide very strong constraints on bulk models. If, for example, only gauge bosons propagate in the bulk but the fermions are localised on the IR brane then the couplings of the gauge boson Kaluza–Klein (KK) modes to the IR-localised fermions yield unacceptably large contributions to T and S and this gives a lower bound of 25 TeV on the mass of the first KK mode of the gauge boson. Of course, one way to relax this bound is to localise the fermions in the bulk and especially the light fermions close to the UV brane and this significantly reduces the constraint coming from the S-parameter. But the T parameter constraints require further attention. One way to handle this [12,13] is by enlarging the gauge symmetry in the bulk to $SU(3)_c \times SU(2)_L \times SU(2)_R \times U(1)_y$ which is an enlarged custodial symmetry which is broken on the IR brane to recover the SM gauge group. It turns out that the corrections to the T parameter coming from the dangerous KK gauge boson sector can be tamed using this custodial symmetry and by a judicious choice of the fermion representations under the extended gauge group it is also possible to rein in the non-oblique $Z \to b\bar{b}$ corrections and eventually the bound on the lightest KK gauge boson mode comes down to about 3 TeV [14,15].

An alternate proposal to address the issue of the T parameter [16,17] uses a deformed metric near the IR brane along with moving the Higgs scalar into the bulk. For this setup, the function $A(y)$ in Eq. (2) is then modified to

$$A(y) = ky - \frac{1}{\nu^2}\log(1 - \frac{y}{y_s}). \tag{3}$$

The UV brane, similar to the RS setup, is located at $y = 0$. The IR brane is however located at $y = y_1$ with the position of the singularity ($y = y_s$) located behind the IR brane at $y_s = y_1 + \Delta$, where $\Delta \sim \frac{1}{k}$. y_1 is determined by demanding the solution to the hierarchy problem which requires $A(y_1) \sim 35$. The limit $\nu \to 0$ reverts to the original RS geometry in Eq. (2). The deformation of the metric actually causes the Higgs field to be moved further away from the IR brane but the gauge boson KK modes are moved by the deformation towards the IR brane. This differential action causes the overlap of the Higgs and KK gauge boson modes to be reduced and that relaxes the bounds coming from the T parameter and the mass of first KK gauge boson mode in this model can be as small as 1.5 TeV [15].

2. Kaluza–Klein gluons and collider searches

In typical Bulk RS models, the lightest KK excitations are those of the gauge bosons and searches for these are likely to be the most promising probes of such a model. Of these, the KK gluons, because of their larger couplings, are the most interesting though there are interesting signals from KK excitations of electroweak gauge bosons and fermions.

In the custodial models, the couplings of the g_{KK} to the SM states [18] are parametrised in terms of the parameter $\xi \equiv \sqrt{kL} \sim 5$ and relative to the QCD coupling g_s are given as:

$$g^{q\bar{q}g_{KK}} \approx \frac{1}{\xi} g_s, \quad g^{Q\bar{Q}^3 g_{KK}} \approx 1 g_s,$$
$$g^{t_R \bar{t}_R g_{KK}} \approx \xi g_s, \quad g^{ggg_{KK}} = 0. \tag{4}$$

These denote the coupling of the first Kaluza–Klein mode of the gluon to light quarks, to the third-generation left-handed doublet, to the right-handed top quark and to the gluon, respectively. Note that the g_{KK} couples predominantly to the right-handed top quark and, consequently, the $g_{KK} \to t\bar{t}$ branching ratio is more than 90%. For the deformed metric the couplings are similar except for overall factors to be discussed later.

Also one sees that the coupling of the g_{KK} to the zero-mode Standard Model gluons vanishes because of the orthonormality of the Kaluza–Klein modes. This means that, at leading order, g_{KK} production takes place via annihilation of light quarks, to which the coupling of the g_{KK} is suppressed and, consequently, the cross-section is small especially since electroweak precision constraints require the mass of the g_{KK} to be not less than 2–3 TeV. The produced g_{KK} decays into a $t\bar{t}$ pair and this tiny cross-section has to compete with a huge QCD $t\bar{t}$ production background. The fact that this is a resonant cross-section helps somewhat but then the g_{KK} has a very large width, owing to its strong coupling to the tops, and so the resonant bump is not sharp but rather smeared out. The fact that the g_{KK} couples chirally to the tops is, however, an advantage and a forward–backward asymmetry to pick out the signal may be used. However, in a pp machine like the LHC this is not easy. Finally, since the t and the $\bar{t}$ come from the decay of a heavy object not less than 2–3 TeV in mass, they are highly boosted. These boosted top jets can effectively be used as signal discriminant [18,19].

Nonetheless, given the smallness of the cross-section it becomes important to look for other production mechanisms for the g_{KK}, especially the ones which have gluon initial states. The associated production of g_{KK} with a $t\bar{t}$ pair leading to distinctive four-top final states (with two boosted tops) is a process that has been studied with this in mind [20–23]. The production of g_{KK} through top loops has also been considered [24] though the loop-contributions are greatly suppressed. Model independent analysis for the searches of colour octet states (colorons) were considered in [25,26].[2]

3. Associated jet production

In this paper, we are proposing the production of a g_{KK} with associated jets (a light quark or gluon jet) in order to complement the leading order g_{KK} production and increase the sensitivity for the g_{KK} at the LHC. At the parton level, the most important contribution is the one where g_{KK} is produced in association with a single hard parton. Top row in Fig. 1 shows few of the contributing diagrams for this process. As this appears at an order of α_s higher than the leading-order g_{KK} production, one would think that the cross-section is smaller. Effects of PDF do partly compensate for the suppression due to α_s. In addition, the associated jet production process has both $q\bar{q}$ and qg initial states and a larger number of sub-process contributions. Consequently, the cross-section for

[2] The phenomenology of such models have been studied in [27–29].

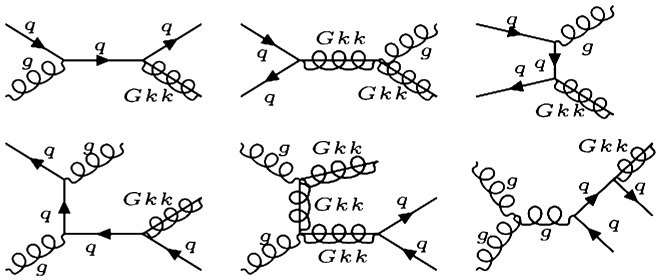

Fig. 1. The subprocesses contributing to g_{KK} production in association with partons. Top row is the g_{KK} production in association with a single parton and the bottom row is the production in association with two partons.

Table 1
Comparison for cross-sections for mass range in normal RS model.

g_{KK} mass (GeV)	LO cross-section (fb)	Associated production (AP) (fb)	AP/LO
2500	169.1	107.6	0.636
3000	52.53	33.28	0.634
3500	17.4	10.99	0.632
4000	5.993	3.723	0.621
4500	2.096	1.277	0.609

Table 2
Comparison for cross-sections for mass range in deformed RS model.

g_{KK} mass (GeV)	LO cross-section (fb)	Associated production (AP) (fb)	AP/LO
1500	1127	695.5	0.617
2000	257.8	162.1	0.629
2500	71.42	45.51	0.637
3000	22.19	14.09	0.635
3500	7.362	4.617	0.627

this process is comparable to the leading-order g_{KK} production process. Tables 1 and 2 give a comparison for the LO cross-section with the cross-section with associated partons for the normal RS and deformed RS models respectively.

We would like to emphasise that, unlike in Refs. [24,30,31], we are not doing the full NLO analysis here since we are concentrating on hard scattering processes and include only real emission.

The g_{KK} produced via the diagrams shown in Fig. 1 will decay predominantly to tops. The tops so produced will decay to a b and a W which will finally result in a multi-jet final state with the associated jet being one of these jets. A detailed analysis of the signal and background, including hadronisation and jet reconstruction is presented in the following section. We will, however, make a couple of points here before proceeding to the discussion of the detailed analysis.

In trying to include final states with more than one jet, we are going to higher orders in QCD perturbation theory. One may wonder then whether we need to include virtual corrections and worry about soft and collinear singularities. We do not have to include these corrections because we are ensuring hard jets in our process. Moreover, some part of the infrared issues are handled by the showering in PYTHIA [32] (albeit in a model-dependent way) and by the matching of the hard amplitude computation with the results of PYTHIA that we have taken into account in a careful manner. If there is any residual doubt about our calculational procedure, it is best to bear the analogy with the Drell–Yan process in mind. The leading-order Drell–Yan process, like leading-order g_{KK} production, is a $q\bar{q}$-initiated process. When we consider the high-p_T Drell–Yan process, in which we consider a single jet recoiling against the lepton–antilepton pair, then as in our case, the qg process kicks in. If we were to ask for two hard jets to be produced in association with the lepton–antilepton pair, then the gg process also comes in. In computing these hard-scattering amplitudes contributing to high-p_T Drell–Yan, we do not have to worry about the soft or collinear singularities because we have ensured that the produced jets are hard. Our process is similar, at the level of the partonic processes, to high-p_T Drell–Yan (and differs from it only in the kinematics peculiar to the production of a heavy particle like the KK gluon) and we are, therefore, justified in neglecting the soft and collinear singularities in our calculation.

Additionally, we calculated the squared matrix-elements for the subprocesses shown in Fig. 1 explicitly and computed the cross-sections, using a parton-level Monte Carlo. This provided us a quick estimate of the cross-section and justified our intuition about its magnitude. It also provided us a rough comparison with the more detailed analysis that we did using MADGRAPH [33] and PYTHIA [32].

Again, while we postpone the detailed discussion of the choice of kinematic cuts to the next section, it is useful to note here some features of the kinematics, arising due to the production of a very massive object at the LHC energies. We are interested in producing a g_{KK}, at least 1.5 TeV or so in mass, in association with a jet. Even at the highest energies at the LHC now available the sub-process centre-of-mass energy will be sufficient only to produce the g_{KK} with small momentum with the p_T-balancing associated jet also, therefore, possessing a p_T that is not very large. When the g_{KK} decays into the $t\bar{t}$ pair, the t and $\bar{t}$ are produced almost back-to-back. But the t and the $\bar{t}$ so produced will be highly boosted and give rise to very collimated hadronic decay products. The small magnitude of the g_{KK} p_T also implies that the recoiling parton carries small net p_T which also poses a challenge in trying to distinguish it from the other hadronic environment. The resultant final state has a g_{KK} + several jets which could arise from partonic subprocesses with more than one associated parton. We therefore also take into account the cross-section due to processes with additional partons. The process with two additional partons arises also from gg initial states (in addition to the $q\bar{q}$ and qg channels) which contribute at the lower orders. The bottom row in Fig. 1 shows the production of g_{KK} in association with two partons. The cross-section is again not very suppressed. Processes with larger number of partons in association will follow the usual perturbation theory pattern and are expected to be suppressed. Further processes with more than two partons will have a tendency to produce softer jets which may not pass the cuts. We have checked the cross-section for g_{KK} with one, two and three additional partons in MADGRAPH and find the above expectation to be borne out. We therefore include the contribution of one parton and two parton sub-processes to the signal cross-section.

4. Signal and background simulations

The signal is characterised by a massive RS KK-gluon (g_{KK}) produced in association with hard partons. The g_{KK} then decays dominantly into a $\bar{t}t$ pair leading to the following signal topology

$$p\,p \to g_{KK} + a \quad \text{or} \quad p\,p \to g_{KK} + a + b \tag{5}$$

where a, b are partons and $g_{KK} \to t\bar{t}$. The requirement of an additional hard parton does not change the signal. This process is at the next to leading order compared to the following leading order (LO) topology

$$p\,p \to g_{KK} \to \bar{t}t. \tag{6}$$

In comparison the g_{KK} produced in a LO process will be almost at rest. The parton-level amplitudes for both the signal and the background were generated using MADGRAPH [33] at 13 TeV centre of mass energy using parton distribution function NNLO1 [34]. The model files have been generated using FEYNRULES [35]. The signal events were generated by adding the following amplitudes:

$$\mathcal{M}_{signal} = \mathcal{M}(pp \to g_{KK}) + \mathcal{M}(pp \to g_{KK} + a) + \mathcal{M}(pp \to g_{KK} + a + b). \quad (7)$$

The most dominant backgrounds are $t\bar{t} + jets$ and QCD. The events for the former is generated by adding the following amplitudes at the parton level:

$$\mathcal{M}_{bg} = \mathcal{M}(pp \to t\bar{t}) + \mathcal{M}(pp \to t\bar{t} + a) + \mathcal{M}(pp \to t\bar{t} + a + b). \quad (8)$$

The QCD background is simulated by adding the following amplitudes at the parton level

$$\mathcal{M}_{bg} = \mathcal{M}(pp \to a + b) + \mathcal{M}(pp \to a + b + c). \quad (9)$$

The associated partons for the $t\bar{t}$ and the signal are required to have a minimum transverse momentum of 50 GeV. A softer cut enhances the background cross-section and hence not desirable. The signal cross-section on the other hand is not drastically affected as the associated parton is expected to have a fairly large transverse momentum from the recoiling g_{KK}.

We need the 'hard jet' from the matrix elements in the second and third terms in the right hand side of Eq. (7). The 'soft jets' are modelled by emissions off $pp \to g_{KK}$ in the first term generated by PYTHIA 8. This was done by matching the MADGRAPH output to PYTHIA 8 using MLM [36] matching scheme. Subsequently, after showering and hadronisation using PYTHIA 8 we apply the following selection criteria to extract the signal:

Jet selection: Assuming hadronic decay of the top, the final state is characterised by at least 6 partons (including 2 b partons). Jets are reconstructed from these partons by employing FASTJET [37,38] using the *anti-k_T* [39] clustering algorithm and setting the jet radius parameter $R = 0.4$. We accept only those jets which satisfy $|\eta| < 2.5$ and $p_T > 50$ GeV.

Event selection: Leptons are required to satisfy $p_T > 20$ GeV and $\eta < 2.5$. Since we are considering a hadronic decay channel for both the tops, only events with no leptons are accepted. In order to reconstruct the g_{KK} mass from the top decay products, each event is further required to have a minimum of 3 jets. An additional condition on a maximum of 5 jets is imposed which is helpful to reduce the QCD background. Due to the heavy mass of the g_{KK}, the decay products of t are likely to be reconstructed in a single jet. Alternatively, one could have imposed the requirement of a minimum 4 normal jets[3] and 2 b-jets. However the requirement of a minimum of two b jets in each event results in depletion of signal events due to b tagging efficiency. As a result, we do not attempt to segregate the b-like jets to those coming from the W-decay and g_{KK} mass is reconstructed from the 3 leading jets in the event. Fig. 2 shows the invariant mass of 3 leading jets in each event demonstrating a distinct peaking behaviour at 3 TeV which is the mass chosen for the g_{KK}.

Background rejection: For the signal, the top pairs and hence its decay products are likely to be highly boosted owing to large g_{KK} mass. As a result the leading jet (j_0) is likely to have a very large p_T in comparison to that of the background. Fig. 3 shows the p_T distribution for the leading jet for the background (blue and green) and the signal (red). We give a hard cut of 1100 GeV on the leading jet. To increase the statistics for the background in this high p_T region, background events are simulated near the tail end of the p_T spectrum. This is implemented by demanding the sum of p_T of the associated partons for background simulation is 1250 GeV.

[3] Jets which are not identified as b-jets.

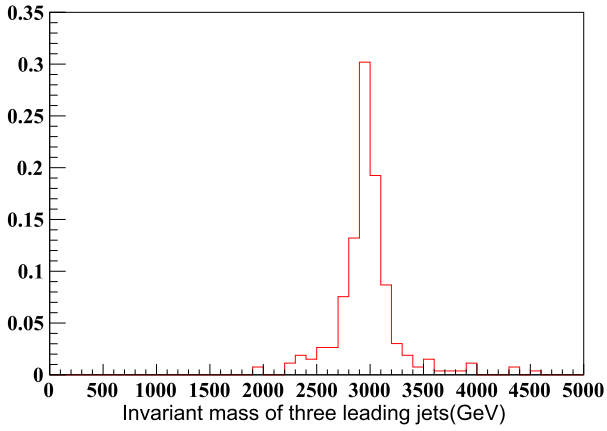

Fig. 2. Reconstructed mass of the g_{KK} from the three leading jets where the mass of g_{KK} is chosen to be 3 TeV.

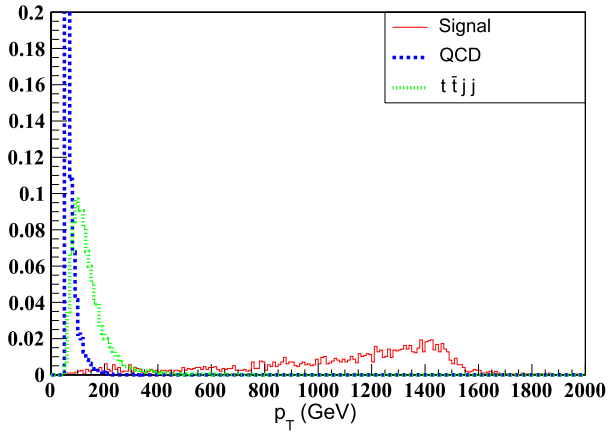

Fig. 3. p_T distribution for the leading jet for the signal (red) and background (blue) for $m_{g_{KK}} = 3$ TeV. (For interpretation of the references to colour in this figure, the reader is referred to the web version of this article.)

Further, each event is required to have a minimum of two and a maximum of 8 jets. In spite of such a hard cut on the leading jet, contamination due to QCD processes is non-zero due to its significant production cross-section. Traditional kinematic cuts prove insufficient to get a significant signal sensitivity.

In this case, studying the jet substructure is extremely useful in eliminating the background to a great extent. It was pointed out earlier that the leading jet for the signal is primarily composed of top decay products. As a result it has a three-lobed structure. This is in sharp contrast to QCD which is one-lobed. A useful way to quantify the number of lobes for a given jet is by considering a variable called *N-subjettiness* [40,41] defined as:

$$\tau_N = \frac{\sum_k p_{T_k} \times \min(\Delta R_{1k}, \Delta R_{2k} \ldots \Delta R_{Nk})}{\sum p_{T_k} \times R} \quad (10)$$

where k runs over the jet constituents and p_{T_k} is the transverse momentum for the k-th constituent. In the above definition, assuming there are N candidate subjets, ΔR_{lk} is the distance in the rapidity–azimuth plane between the k-th constituent and the l-th candidate subjet. For a jet with N-distinct lobes of energy, all the radiation inside the jet will be aligned along their direction, which is the same as the direction of the candidate subjet. As a result each constituent of a jet will be clustered with one of its subjets and one can expect the $\min(\Delta R_{1k}, \Delta R_{2k} \ldots \Delta R_{Nk})$ to be closer to zero. Thus, $\tau_N \to 0$ for N-lobe configuration while $\tau_{N-1} > \tau_N$ for $N > 1$. In this case τ_{N+1} is expected to be comparable to τ_N. For

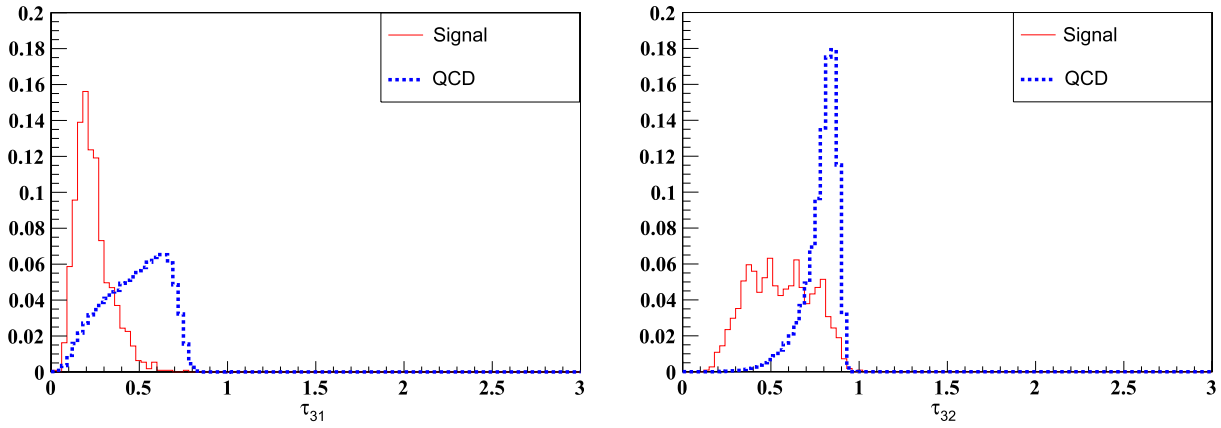

Fig. 4. Subjettiness ratio τ_{31} on the left and τ_{32} on the right for both signal and background.

Table 3
Cut flow table for $m_{g_{KK}} = 3$ TeV.

Ser.No.	Cuts	QCD ($p_T^{sum} > 1250$)	$t\bar{t}jj$ ($p_T^{sum} > 1250$)	Signal events
1	Given number of events	10^7	10^5	10000
2	Cross-section (fb)	720×10^3	132	94.2
3	$n_{lepton} = 0$	9203793	39386	3122
4	$p_T^{j_0} > 1100$ GeV	233520	14051	1363
5	Subjettiness cut	262	218	265
6	$\lvert m_{g_{KK}} - 3000\rvert < 80$ GeV	48	55	112

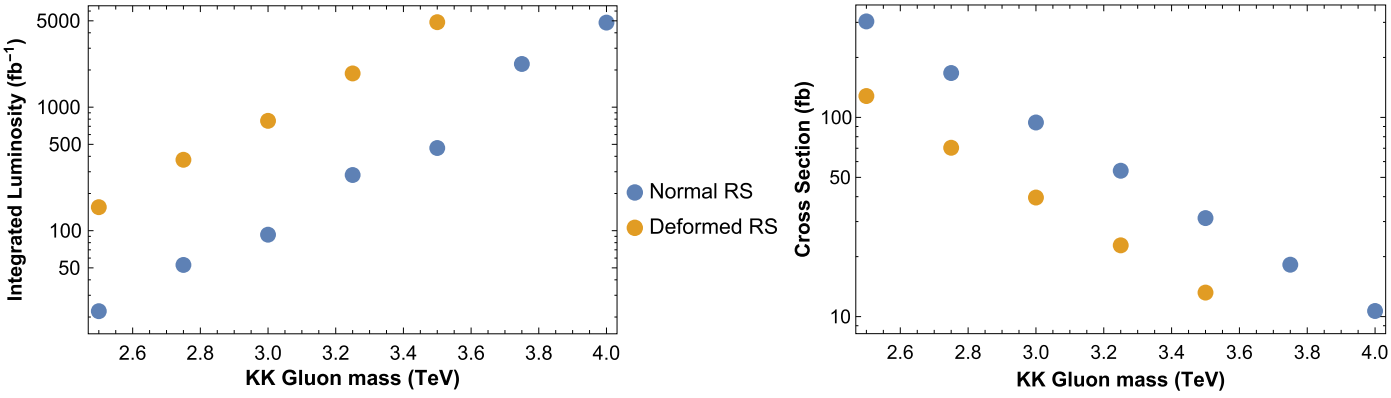

Fig. 5. Minimum luminosity required for a 5σ sensitivity for normal RS (blue) and deformed RS (orange). The right plot shows the production cross-section for the different masses. (For interpretation of the references to colour in this figure, the reader is referred to the web version of this article.)

QCD τ_1 is small while for the signal τ_3 is small. A useful application is to consider ratios $\tau_{N+1,N} = \tau_{N+1}/\tau_N$. For the scenario under consideration, we evaluate τ_{32} and τ_{31}. Both these ratios are expected to be smaller for the signal than QCD as shown in Fig. 4. One of the most dominant background to the signal is $t\bar{t}$ + jets production via SM processes due to its significant production cross-section. It is therefore essential to suppress this background significantly to have sufficient signal over background efficiency for luminosities attainable in the near future. We select $\tau_{31} < 0.35$ and $\tau_{32} < 0.35$ for the leading jet. Further we also impose a cut of $\tau_{21} < 0.6$ on the sub-leading jet.

Results: Table 3 gives the summary of the number of events passing various cuts at each level for both the signal and background. These results correspond to $m_{g_{KK}} = 3$ TeV. The cuts are optimised for this particular mass. As explained earlier events with zero leptons are accepted to facilitate hadronic decay of the top. A hard cut on the transverse momentum of the leading jet (j_0) drastically reduces the $t\bar{t}$ background without affecting the signal significantly. With this set of cuts, $\sim 5\sigma$ sensitivity can be obtained for a minimum luminosity of 90 fb^{-1} for $m_{g_{KK}} = 3$ TeV.

We repeat the analysis above for different masses of the g_{KK} and we follow exactly the same pattern of cuts as in Table 3. The background events are simulated differently for different masses of g_{KK}. In the sixth line of Table 3 we have used a mass cut around different KK-gluon masses. As a result we extract background events around different invariant mass bins for the three leading jets, each corresponding to the benchmark masses used to simulate the signal.

In Fig. 5 we present results for both normal and deformed RS models. For the normal RS model we assume 92% branching fraction into $t\bar{t}$ pair, while for the deformed model we assume 83% branching fraction [42]. Left plot in Fig. 5 presents the minimum luminosity required for a 5σ signal sensitivity for the different masses for both normal RS and deformed RS models. Owing to constraints from precision electroweak data we do not consider masses below 2.5 TeV for normal RS model. Due to their larger production cross-section, the lower masses (indicated by blue points in the figure) have better sensitivity in terms of early discovery prospects.

Lower masses can be admitted in a deformed RS model. For the deformed model we choose $\nu = 0.4$ while the curvature radius is chosen to be $L_1 = 0.2/k$ [42,43]. This scenario however suffers from reduced production cross-section owing to the smaller coupling of the g_{KK} to the lighter quarks which is roughly $0.13 g_s$.

For both scenarios, we use a very hard cut on the transverse momentum of the leading jet, $p_T^{j_0} > 1100$ GeV in Table 3. Since the p_T of the leading jet is $\sim m_{g_{KK}}/2$, this cut is more effective for the heavier masses as compared to the lighter masses. While this depletes majority of the signal points for 2 TeV KK gluon, this is helpful in depleting the background to a great extent.

5. Conclusion

Search for KK excitations of the gluons in warped framework is interesting due to their relatively large production cross-section in comparison to other KK states. Their masses are, however, strongly constrained due to limits from electroweak precision data. This necessitates the need for an effective strategy to probe relatively heavy states in the Run II of LHC. We consider a process where the g_{KK} is produced in association with jets. We consider a simple set of cuts to extract the signal from the background. The signal is characterised by highly collimated leading jets owing to the massive nature of g_{KK}. Cuts as strong as 1100 GeV are imposed on the p_T of the leading jet without adversely affecting the number of signal sensitivity. We present results for both the normal RS model and the deformed RS model. In normal RS, g_{KK} as heavy as 3 TeV can be probed in the Run II of the LHC with luminosities ~ 90 fb^{-1} while masses as heavy as 4 TeV can be accessed in the HL-LHC. For the deformed case masses ~ 2.5 TeV are accessible in the current run of LHC. The sensitivity to 3 TeV masses can be probed in the HL-LHC.

While this simple cut based analysis is highly effective, it would be interesting to find alternate strategies so that one can explore the heavy mass regime more efficiently. The observation of highly collimated decay products of either top coming from the g_{KK} provides strong motivation to study the jet-substructure in greater detail and constitutes work for the future.

Acknowledgements

We would like to thank Monoranjan Guchait for the extensive discussions and immensely useful inputs on the collider analysis. We are also grateful to him for the going through the manuscript in detail and for his suggestions on improving the quality of the draft. AMI would like to thank Amit Chakraborty for discussions on simulations. NM would like to thank the Department of Theoretical Physics, TIFR for computational resources. We would also like to acknowledge the contributions of Sophie Renner to the initial stages of this work.

The authors would like to dedicate this paper to the memory of Guido Altarelli.

References

[1] L. Randall, R. Sundrum, A large mass hierarchy from a small extra dimension, Phys. Rev. Lett. 83 (1999) 3370–3373.
[2] H. Davoudiasl, J.L. Hewett, T.G. Rizzo, Bulk gauge fields in the Randall–Sundrum model, Phys. Lett. B 473 (2000) 43–49.
[3] A. Pomarol, Gauge bosons in a five-dimensional theory with localized gravity, Phys. Lett. B 486 (2000) 153–157.
[4] T. Gherghetta, A. Pomarol, Bulk fields and supersymmetry in a slice of AdS, Nucl. Phys. B 586 (2000) 141–162.
[5] Y. Grossman, M. Neubert, Neutrino masses and mixings in nonfactorizable geometry, Phys. Lett. B 474 (2000) 361–371.
[6] T. Gherghetta, TASI lectures on a holographic view of beyond the standard model physics, in: C. Csaki, S. Dodelson (Eds.), Physics of the Large and the Small, Proceedings of the Theoretical Advanced Study Institute in Elementary Particle Physics, TASI 2009, 2010.
[7] G. Burdman, Flavor violation in warped extra dimensions and CP asymmetries in B decays, Phys. Lett. B 590 (2004) 86–94.
[8] S.J. Huber, Flavor violation and warped geometry, Nucl. Phys. B 666 (2003) 269–288.
[9] S. Casagrande, F. Goertz, U. Haisch, M. Neubert, T. Pfoh, Flavor physics in the Randall–Sundrum model: I. Theoretical setup and electroweak precision tests, J. High Energy Phys. 0810 (2008) 094.
[10] M. Bauer, S. Casagrande, U. Haisch, M. Neubert, Flavor physics in the Randall–Sundrum model: II. Tree-level weak-interaction processes, J. High Energy Phys. 1009 (2010) 017.
[11] K. Agashe, G. Perez, A. Soni, Flavor structure of warped extra dimension models, Phys. Rev. D 71 (2005) 016002.
[12] K. Agashe, A. Delgado, M.J. May, R. Sundrum, RS1, custodial isospin and precision tests, J. High Energy Phys. 0308 (2003) 050.
[13] K. Agashe, R. Contino, L. Da Rold, A. Pomarol, A custodial symmetry for Zb anti-b, Phys. Lett. B 641 (2006) 62–66.
[14] H. Davoudiasl, S. Gopalakrishna, E. Ponton, J. Santiago, Warped 5-dimensional models: phenomenological status and experimental prospects, New J. Phys. 12 (2010) 075011.
[15] A.M. Iyer, K. Sridhar, S.K. Vempati, Bulk RS models, electroweak precision tests and the 125 GeV Higgs, Phys. Rev. D 93 (7) (2016) 075008.
[16] J.A. Cabrer, G. von Gersdorff, M. Quiros, Warped electroweak breaking without custodial symmetry, Phys. Lett. B 697 (2011) 208–214.
[17] J.A. Cabrer, G. von Gersdorff, M. Quiros, Suppressing electroweak precision observables in 5D warped models, J. High Energy Phys. 05 (2011) 083.
[18] K. Agashe, A. Belyaev, T. Krupovnickas, G. Perez, J. Virzi, LHC signals from warped extra dimensions, Phys. Rev. D 77 (2008) 015003.
[19] B. Lillie, L. Randall, L.-T. Wang, The bulk RS KK-gluon at the LHC, J. High Energy Phys. 0709 (2007) 074.
[20] M. Guchait, F. Mahmoudi, K. Sridhar, Associated production of a Kaluza–Klein excitation of a gluon with a t anti-t pair at the LHC, Phys. Lett. B 666 (2008) 347–351.
[21] B. Lillie, J. Shu, T.M.P. Tait, Top compositeness at the Tevatron and LHC, J. High Energy Phys. 04 (2008) 087.
[22] A. Pomarol, J. Serra, Top quark compositeness: feasibility and implications, Phys. Rev. D 78 (2008) 074026.
[23] G. Servant, Four-top events at the LHC, in: Physics at the LHC2010, Proceedings, 5th Conference, PLHC2010, Hamburg, Germany, June 7–12, 2010, 2010, pp. 254–257.
[24] B.C. Allanach, F. Mahmoudi, J.P. Skittrall, K. Sridhar, Gluon-initiated production of a Kaluza–Klein gluon in a bulk Randall–Sundrum model, J. High Energy Phys. 1003 (2010) 014.
[25] R.S. Chivukula, A. Farzinnia, E.H. Simmons, R. Foadi, Production of massive color-octet vector bosons at next-to-leading order, Phys. Rev. D 85 (2012) 054005.
[26] R.S. Chivukula, A. Farzinnia, J. Ren, E.H. Simmons, Hadron collider production of massive color-octet vector bosons at next-to-leading order, Phys. Rev. D 87 (9) (2013) 094011.
[27] R.S. Chivukula, A. Farzinnia, J. Ren, E.H. Simmons, Constraints on the scalar sector of the renormalizable coloron model, Phys. Rev. D 88 (7) (2013) 075020; Phys. Rev. D 89 (5) (2014) 059905 (Erratum).
[28] R.S. Chivukula, E.H. Simmons, A. Farzinnia, J. Ren, LHC constraints on a Higgs boson partner from an extended color sector, Phys. Rev. D 90 (1) (2014) 015013.
[29] R.S. Chivukula, A. Farzinnia, E.H. Simmons, Vacuum stability and triviality analyses of the renormalizable coloron model, Phys. Rev. D 92 (5) (2015) 055002.
[30] P. Mathews, V. Ravindran, K. Sridhar, W.L. van Neerven, Next-to-leading order QCD corrections to the Drell–Yan cross section in models of TeV-scale gravity, Nucl. Phys. B 713 (2005) 333–377.
[31] P. Mathews, V. Ravindran, K. Sridhar, NLO-QCD corrections to dilepton production in the Randall–Sundrum model, J. High Energy Phys. 10 (2005) 031.
[32] T. Sjostrand, S. Mrenna, P.Z. Skands, A brief introduction to PYTHIA 8.1, Comput. Phys. Commun. 178 (2008) 852–867.
[33] J. Alwall, R. Frederix, S. Frixione, V. Hirschi, F. Maltoni, O. Mattelaer, H.S. Shao, T. Stelzer, P. Torrielli, M. Zaro, The automated computation of tree-level and next-to-leading order differential cross sections, and their matching to parton shower simulations, J. High Energy Phys. 07 (2014) 079.
[34] R.D. Ball, et al., Parton distributions with LHC data, Nucl. Phys. B 867 (2013) 244–289.
[35] A. Alloul, N.D. Christensen, C. Degrande, C. Duhr, B. Fuks, FeynRules 2.0 — a complete toolbox for tree-level phenomenology, Comput. Phys. Commun. 185 (2014) 2250–2300.
[36] M.L. Mangano, M. Moretti, F. Piccinini, R. Pittau, A.D. Polosa, ALPGEN, a generator for hard multiparton processes in hadronic collisions, J. High Energy Phys. 07 (2003) 001.
[37] M. Cacciari, FastJet: a code for fast k_t clustering, and more, in: Deep Inelastic Scattering, Proceedings, 14th International Workshop, DIS 2006, Tsukuba, Japan, April 20–24, 2006, 2006, pp. 487–490.

[38] M. Cacciari, G.P. Salam, G. Soyez, FastJet user manual, Eur. Phys. J. C 72 (2012) 1896.
[39] M. Cacciari, G.P. Salam, G. Soyez, The anti-k_t jet clustering algorithm, J. High Energy Phys. 04 (2008) 063.
[40] J. Thaler, K. Van Tilburg, Identifying boosted objects with N-subjettiness, J. High Energy Phys. 03 (2011) 015.
[41] J. Thaler, K. Van Tilburg, Maximizing boosted top identification by minimizing N-subjettiness, J. High Energy Phys. 02 (2012) 093.
[42] A. Carmona, E. Ponton, J. Santiago, Phenomenology of non-custodial warped models, J. High Energy Phys. 10 (2011) 137.
[43] J. de Blas, A. Delgado, B. Ostdiek, A. de la Puente, LHC signals of non-custodial warped 5D models, Phys. Rev. D 86 (2012) 015028.